Drug distribution in nanostructured lipid particles

Siavash Saeidpour,[1*] Silke B. Lohan,[2*] Agnieszka Solik,[3] Victoria Paul,[2] Roland Bodmeier,[3] Gaith Zoubari,[3] Michael Unbehauen,[4] Reiner Haag,[4] Robert Bittl,[1] Martina C. Meinke,[2] Christian Teutloff,[1§]

[1] *Freie Universität Berlin, Fachbereich Physik, Berlin, Germany*

[2] *Department of Dermatology, Venerology and Allergology, Center of Experimental and Applied Cutaneous Physiology, Charité - Universitätsmedizin Berlin, Germany*

[3] *Freie Universität Berlin, College of Pharmacy, Berlin, Germany*

[4] *Freie Universität Berlin, Institut für Chemie und Biochemie, , Berlin, Germany*

*both authors contributed equally

[§]Corresponding author: christian.teutloff@fu-berlin.de, phone +493083853394, Arnimallee 14, 14195 Berlin, Germany

Final version: https://doi.org/10.1016/j.ejpb.2016.10.008

Abstract

The targeted design of nanoparticles for efficient drug loading and defined release profiles is even after 25 years of research on lipid-based nanoparticles still no routine procedure. It requires detailed knowledge about the interaction of the drug with the lipid compounds and about its localisation and distribution in the nanoparticle. We present here an investigation on nano-sized lipid particles (NLP) composed of Gelucire and Witepsol as solid lipids, and Capryol as liquid lipid, loaded with Dexamethasone, a glucocorticoid used in topical treatment of inflammatory dermal diseases. The interactions of Dexamethasone, which was spinlabelled by 3-(Carboxy)-2,2,5,5-tetramethyl-1-pyrrolidinyloxy (DxPCA), with its microenvironment is monitored by EPR spectroscopy at 94 GHz at low temperatures. The mobility of the spin-labelled drug was probed by X-band EPR at room temperature. In order to relate the magnetic and dynamic parameters deduced from EPR to the local environment of the spin probe in the NLP, investigations of DxPCA in the individual lipid compounds were carried out. The magnetic parameters reflecting the polarity of DxPCA's environment as well as the parameters describing the mobility of the drug reveal that in the case of colloidal dispersions of the lipids and also the NLP DxPCA is attached to the surface of the nanoparticles. Although the lipophilic drug is almost exclusively associated to the NLP in aqueous solution, dilution experiments show, that it can be easily released from the nanoparticle.

Keywords

Nanoparticles

Drug delivery system

Dexamethasone

Lipids

Dermal drug delivery

Electron paramagnetic resonance (EPR) spectroscopy

Spinlabel

Chemical compounds studied in this article

Dexamethasone (PubChem CID: 5743); 3-(Carboxy)-2,2,5,5-tetramethyl-1-pyrrolidinyloxy (PubChem CID: 519874); Stearoyl macrogolglycerides (Gelucire® 50/ 13) (PubChem SID: 135354605); Propylene glycol monocaprylate (Capryol® 90) (PubChem CID: 53630264); Witepsol (ChemIDplus: 0091744422)

Introduction

Colloidal systems like suspensions, emulsions and micellar or vesicular solutions are in common use for the topical application of pharmaceuticals with limited water solubility[1]. As an alternative to oil/water emulsions and liposomes, lipid-based nanoparticles have been introduced as drug delivery systems for poorly water-soluble drugs [2, 3]. These nanoparticles have potential advantages over liposomes and emulsions: They show room/body temperature stability, no organic solvents are needed throughout preparation, a broad application spectrum, and the controlled release of the incorporated drug is possible [4, 5]. Additionally the composition of nanoparticles from different lipids and surfactants allows for tuning to different drug solubilities [4, 6, 7].

Lipid-based nanoparticles can be classified into solid lipid nanoparticles (SLN) or heterogeneous, presumably liquid/solid phase matrix particles, called nanostructured lipid carriers (NLC). NLC were developed to increase the loading capacity compared to SLN [4]. A number of investigations concerning the size and shape of SLN and NLC has been published [8, 9]. Either a crystalline or supercooled melt matrix core is found, depending on the compositions [8-10].

Investigations concerning the drug distribution within the nanoparticles are rare [10, 11]. One report made use of model compounds like the fluorescent nile red and found a localisation in the oily phase of NLC [12]. Diverging models assume the inclusion of substrates either in the core, the outer shell, as a colloidal dispersion in the lipid matrix or in a homogeneous distribution [13, 14]. It is generally accepted that lipid-based nanoparticles including NLCs improve the penetration of drugs through the skin [5, 15, 16].

For the treatment of inflammatory diseases and in particular dermal diseases Dexamethasone (Dx) is regularly used [17]. It is a synthetic glucocorticoid with anti-inflammatory and immunosuppressive effects [17]. Due to its low solubility in water (89 mg/l at 25 °C) co-solvation or usage of liquid lipids is necessary.

Electron paramagnetic resonance (EPR) is a well-established method for probing the local environment of a spin probe with respect to polarity, proticity and mobility [18, 19]. NO-based spin labels have been used as probes in membrane proteins [20, 21], lipids [18, 19]] and liposomes [22, 23]. EPR can

furthermore provide information on the loading of molecules onto, localisation in and release from nano-sized carrier systems [11, 24-26].

In the present study, multi-frequency EPR was used to determine the microenvironment of the spin-labeled Dx within lipid-based carrier systems to elucidate the localisation of the drug within the carrier. Control measurements were performed on different sizes of the NLP, on its individual compounds and mixtures at room temperature and under cryogenic conditions (80 K). Furthermore, dilution experiments were performed to study the release kinetics and particle stability.

Material and Methods

Preparation of spin-labelled dexamethasone (DxPCA)

DxPCA was synthesized by refluxing Dx with PCA, 4-(Dimethyl)-aminopyridin and 1-Ethyl-3-(3-dimethylaminopropyl) carbodiimide in dichloromethane for 3h with subsequent column-chromatographic purification [27].

Synthesis of nano-sized lipid particles (NLP)

The lipid components Gelucire® 50/13 (stearoyl macrogolglycerides,GATTEFOSSÉ GmbH, Bad Krozingen, Germany), Witepsol® S55 (solid triglycerides containing hydrogenated coco-glycerides, beeswax and ceteareth-25, CREMER OLEO GmbH & Co. KG, Hamburg, Germany), and Capryol® 90 (propylene glycol monocaprylate, Gattefossé GmbH, Bad Krozingen, Germany) were mixed in a ratio of 5:3:1 (w/ w) and melted at 60°C together with 0.5% (w/ w) PCA-labeled Dx. The 10% (w/ w) lipid nanosuspension was prepared from a nanoemulsion by pouring ultrapure water of the same temperature to the lipid melt and high-shear-homogenization for 5 minutes. Finally, the nanoemulsion was cooled to room temperature to solidify the lipid phase and thus, to obtain the lipid nanosuspension. The lipid nanosuspension was filtered through 0.7 µm glass fiber filters (Whatman® GF/F; Sigma-Aldrich Chemie GmbH, Steinheim, Germany) to eliminate precipitated drug crystals from the water phase.
Two different sizes of DxPCA loaded NLP were produced to study the effect of loading. Furthermore, DxPCA was incorporated into single lipid components of the NLP and in selected lipid combinations, with and without dispersion in water to associate the microenvironment of DxPCA in the NLP.

Particle size determination

The mean particle size of the NLP was determined by a Zetasizer® Nano ZS (Malvern Instruments GmbH, Herrenberg, Germany) equipped with a He-Ne laser (633 nm) at a backscattering angle of 173°C and cell temperature of 25°C. The lipid nanosuspension was diluted to a ratio of 1:10 (v/v) with ultrapure water. 10 runs were performed, from which the mean particle size and polydispersity index with standard deviation was calculated. The particle size of the DxPCA NLP is 134 ± 3 and 242 ± 18 nm, respectively.

To investigate the release behaviour of DxPCA, dilution series were performed: a NLP solution (NLP diameter: 134 nm ± 3 nm) loaded with DxPCA was diluted to ratios of 1:10 and 1:50 with water, followed by measurements with a Zetasizer® Nano ZS.

Electron paramagnetic resonance (EPR) spectroscopy

Cryogenic temperature (80K) EPR measurements were performed using a W-band (94 GHz) EPR spectrometer (Bruker Elexsys E680 S/W-Band) equipped with a Teraflex EN600-1021H probe head (Bruker Biospin, Karlsruhe, Germany). Room temperature measurements at X-band (9 GHz) were performed on a lab-built spectrometer employing a SHQ probe head (Bruker Biospin, Karlsruhe, Germany). The temperature was monitored by an Oxford ITC 503 temperature controller. The magnetic field was calibrated using a $N@C_{60}$ standard [28].

For all cryogenic measurements the samples were prepared in quartz tubes of 0.87/0.7 mm (outer diameter (o.d.)/inner diameter (i.d.) (VitroCom Inc, Mountain Lakes, USA) for W-band. Room temperature EPR at X-band was performed with 2 mm/1mm (o.d./i.d.) capillaries. The experimental parameters are different for each microwave band and are shown in the respective figure legend.

The evaluation of the magnetic parameters (g-matrix, ^{14}N hyperfine couplings, rotational correlation time and line width) for determining the environment polarity and mobility of DxPCA was performed using the EasySpin toolbox [29], a Matlab package **(**The MathWorks GmbH, Ismaning, Germany) for EPR spectra simulation.

Results

Localisation of DxPCA within the NLP

DxPCA was investigated in NLP and in different lipid-solutions of the NLP components by X-band (9.4 GHz) and W-band (94 GHz) at room temperature and at 80 K to evaluate the microenvironment properties polarity and viscosity, and the mobility of the drug in the used carrier system.

The g-matrix principal value g_{xx} and the ^{14}N hyperfine coupling parameter A_{zz} are sensitive to the polarity and proticity of the microenvironment of a nitroxide compound [30, 31]. To study the *g*-matrix and ^{14}N hyperfine coupling, DxPCA loaded to NLP was investigated by high frequency (W-band) EPR spectroscopy at 80 K (Figure 1). Figure 1 shows the low temperature spectra of DxPCA in aqueous dispersions of Gelucire/Witepsol, in NLP (242 nm), in the liquid lipid Capryol, and of DxPCA dissolved in water. Additionally EPR spectra of DxPCA in Gelucire, Witepsol, Gelucire/Witepsol mixture and Gelucire/water dispersion were recorded and are shown in Figure S1. Water was chosen as a reference, since it acts as the solvent surrounding the NLP and has one of the highest polaritiy and proticity properties [32]. The g-matrix and the ^{14}N hyperfine coupling matrix A of DxPCA in the different mixtures/solvents were evaluated by simulation of the experimental spectra and are given in Table 1. Thereof, the principal components g_{xx} and A_{zz} are most sensitive to the solvent properties' polarity and proticity which are indicated in Figure1.

Table 1 Magnetic interaction parameters of DxPCA in NLP, water and different lipids

DxPCA surrounded by	g-matrix principal values (SD)			Hyperfine Coupling (*hfc*) (MHz)		
	g_{xx}	g_{yy}	g_{zz}	A_{xx}	A_{yy}	A_{zz}
water	2.0081(2)	2.0060(2)	2.0021(5)	14	13	104
NLP (242nm)	2.0085(3)	2.0060(2)	2.0021(1)	15	15	99
Gelucire	2.0090(3)	2.0062(3)	2.0021(2)	13	13	95
Witepsol	2.0090(5)	2.0062(4)	2.0021(3)	12	10	95
Capryol	2.0087(2)	2.0061(5)	2.0021(4)	13	13	98
Gelucire(water)	2.0088(4)	2.0062(3)	2.0022(2)	14	12	97
Gelucire/Witepsol	2.0090(2)	2.0062(5)	2.0021(2)	12	13	95

Gelucire/Witepsol(water)	2.0086(5)	2.0061(5)	2.0021(5)	14	15	98

The g_{xx}- and A_{zz}-values of DxPCA in water are typical for a spin label in an aqueous environment [31]. All g_{xx}-values for DxPCA in the lipids are upshifted and all A_{zz} are downshifted compared to the water solution, as expected for these more lipophilic and less protic environments. DxPCA in the solid lipids display the most upshifted g_{xx}- and downshifted A_{zz}-values. DxPCA in the NLP shows values almost identical to those in the liquid lipid Capryol or in a Gelucire/Witepsol mixture dispersed in water. Interestingly, the g-values and ^{14}N-*hfc* for DxPCA depend strongly on the type of preparation. In the pure lipids Gelucire and Witepsol or the Gelucire/Witepsol mixture (Fig S1), the magnetic parameters are shifted towards lower polarity, whereas in the aqueous dispersions of these lipids a clear trend of a shifts towards higher polarity is seen (Table 1). Thus, the spin-labelled drug apparently has to be located in the lipid nanoparticles in an environment such that the magnetic parameters are influenced by the polarity of water.

The line shape of room temperature (*rt*) X-band EPR spectra encodes the mobility of a spin label, here the spin-labelled drug DxPCA, and thereby reports on the viscosity of its environment (Figure 2, Figure S2). The mobility can be parameterized under the assumption of isotropic rotation by the rotational correlation time (t_{corr}). This parameter was evaluated by simulation of the *rt*-EPR spectra (dashed lines). Figure 2 shows a comparison of *rt* X-band EPR of DxPCA in water, NLP and selected individual lipid compounds. Further spectra in other lipids and lipid mixtures are shown in Figure S2.

The *rt*-EPR spectrum of DxPCA dissolved in water is composed of two components, a spectrum consisting of three narrow lines, and a broad unstructured spectrum underneath the middle line of the narrow line spectrum (Figure 2, last spectrum). The solubility of DxPCA in water is quite limited (approx. 2 µmol/l at *rt*, see also information given in the ESI) and DxPCA is presumably partially aggregated in aqueous solution [33]. The broad spectrum can be attributed to such an aggregated DxPCA fraction (see also [34] for further details). The narrow-line spectrum can be assigned to the dissolved DxPCA fraction. The t_{corr} of the free DxPCA in water derived from the spectrum is approximately 90 ps. DxPCA in NLP shows a superposition of a spectrum with three broadened lines, indicating a

significantly lower mobility of DxPCA (t_{corr}=3.2 ns) [35], and of a minority of free DxPCA directly visible only as a narrow feature at 336.5 mT, The free DxPCA component accounts for only approx. 2 % of the overall intensity. In the liquid lipid Capryol (Figure 2, second spectrum from top) DxPCA is tumbling slower ($t_{corr} \approx$ 1.3 ns) than in water, but significantly faster than in the other lipids. The *rt*-EPR spectrum for DxPCA in the solid Gelucire/Witepsol mixture (Figure 2, top spectrum) is similar to those in the individual lipids (see Figure S2). Interestingly, the *rt*-EPR spectra of DxPCA in a Gelucire/Witepsol dispersion in water (Gelucire/Witepsol(water)) resembles starting from the central peak to the high-field end closely the spectrum observed for the NLP case. The low field side of the Gelucire/ Witepsol spectrum shows two components, one that again closely resembles the spectral shape found for DxPCA in NLP and one arising from a more immobilized fraction (low field peak). The main component of the spectrum can be approximated by a simulation with a single component (t_{corr}=4.5 ns).

In order to analyze whether the NLP size has an effect on the loading with DxPCA, two batches with different sizes (134 and 242 nm) have been investigated. Figure S4 shows the X-band *rt*-EPR spectra of these NLP sizes at identical NLP concentrations. The sample with the 134 nm NLP shows a signal intensity increase by a factor of 1.8 compared to the 242 nm NLP, matching the change of surface to volume ratio of the NLP due to the size change. This is a clear evidence, that the DxPCA molecules are associated with the surface of the nanoparticles.

The release of DxPCA from the nanoparticles was studied in a dilution series of NLP in water (Figure S5). With increasing dilution the linewidth of the low field and the high field peak becomes narrower. Already in the undiluted sample, but most prominent at 1:10 a splitting of the high-field peak into a broad and a narrow component can be seen. The narrow peak increases in intensity with increasing dilution, whereas the broad peak is disappearing. Comparing the narrow-line component with the DxPCA spectrum in water, it becomes clear that this narrow component represents free DxPCA in solution. This indicates an equilibrium between DxPCA associated with the NLP and free DxPCA in solution. With increasing dilution the DxPCA dissociates from the NLP, thereby reestablishing this solvent equilibrium as reflected by the increase of the narrow component relative to the broad one (see Figure S5). A disintegration or decay of the NLP by the dilution has been excluded by size determination of the particles (Figure S6).

Discussion

The magnetic interaction parameters g_{xx}- and A_{zz} obtained by W-band EPR at 80 K (Figure 1, Table 1), which report on the polarity of the spin labelled drug's microenvironment, show that DxPCA loaded to NLP experiences an environment of higher polarity than when dissolved in bulk solid lipids. An environment of similar polarity as for NLP was found for DxPCA in the liquid lipid Capryol, but also as when investigated in Gelucire/Witepsol dispersed in water (Table 1). The higher polarity reported for DxPCA in the NLP compared to the bulk solid lipids could be due to an exclusive localisation of DxPCA in the Capryol fraction of the NLP. However, this explanation is excluded for DxPCA in the Gelucire/Witepsol particles dispersed in water. At least for the Gelucire/Witepsol particles, but eventually also for the NLP, the reported increased environment polarity for DxPCA evidences an influence of water on the magnetic parameters. This could occur either by water incorporated into the nanoparticles due to the substantial amount of polar side chains of Gelucire (OHV=36-56) and Witepsol (OHV=50-65) or by a localisation of DxPCA outside the nanoparticle core at the lipid-water interface at the surface of the particles. A distinction between these two scenarios is impossible based on the effective environment polarity alone.

The distinction whether DxPCA in NLP is in an environment dominated by Capryol or, as in the case of the Gelucire/Witepsol particles, in an environment strongly influenced by water can be made when regarding the DxPCA mobility in the different compounds. The difference in DxPCA mobility is best seen in the *rt*-X-band spectra by the broadening of the high field peak. The EPR spectra show a distinctly reduced mobility of DxPCA in NLP compared to the pure liquid lipid Capryol (Figure 2). This excludes the Capryol fraction as a potential environment of DxPCA within the NLP. Thus, the higher environment polarity seen by DxPCA in NLP compared to the solid lipids must have the same origin as for the Gelucire/Witepsol particles dissolved in water.

The DxPCA mobility can again be used to distinguish between the possible effect of water incorporated into the NLP and the Gelucire/Witepsol particles, or a localisation of DxPCA at the water-exposed particle surface. In case of an effect by incorporated water a similar mobility of DxPCA in the bulk solid lipids, NLP and Gelucire/Witepsol(water) would be expected. However, a much higher mobility of DxPCA in NLP than in the bulk solid lipids is found (Figures 2 and S3) while rather similar mobility is

seen for NLP and Gelucire/Witepsol(water). The slightly higher mobility of DxPCA in NLP than in Gelucire/Witepsol(water) might be due to a softening of the NLP by Capryol. Thus, the observed DxPCA mobility clearly argues against an effect of water incorporated into the NLP as origin of the higher environment polarity experienced by the spin-labelled drug. Taken together the polarity and mobility information leads to the conclusion of a DxPCA location in the outer shell of the NLP.

This conclusion on the DxPCA location in the NLP is corroborated by comparison differently sized NLP (242 nm vs 134 nm) (Figure S3). The smaller particles showed about a two times higher loading capacity of DxPCA per volume, which fits well to the increased surface area-to-volume ratio of 1.8 (scaling with the inversely with the particle size).

Sivaramakrishnan et al. (2004) also demonstrated that glucocorticoids loaded to lipophilic carrier systems are more likely to adhere to the particle surface than to the inner lipid matrix [36]. Furthermore, energy dispersive X-ray analysis has shown that Dx, if loaded to lipid particles, is partially localized at the particle surface [37]. In addition, the dilution experiments of the two NLP batches showed a complete release of DxPCA (Figure S4) by establishing the solution equilibrium between solvent and nanoparticle as reflected by the high mobility EPR spectrum at 1:200 dilution.

Conclusion

The study of DxPCA in the individual compounds of NLP has revealed a remarkable dependence of the microenvironment polarity on the lipid formulation. A colloidal dispersion of the solid lipids in water, which were loaded before dispersion with DxPCA, increases the effective polarity of the environment experienced by the spin-labelled drug. In addition, the mobility of DxPCA differs in the individual lipids, lipid dispersions and the NLP. In the liquid lipid Capryol a rather high mobility of DxPCA is found, while a strong immobilization is found in the pure solid lipids. For NLP and the lipid dispersions an intermediate mobility is observed.

Even though the effective environment polarity experienced by DxPCA is compatible with a solvation by the liquid lipid Capryol within the NLP this can be excluded on the basis of the differing mobility. Important corroboration of this conclusion has been provided by studies on dispersions of solid lipid mixtures without Capryol as reference systens, which show similar effective polarity and mobility as the NLP.

Taken together the polarity and mobility studies by multi-frequency EPR at room and cryogenic temperatures strongly argue for a location of DxPCA at the surface of the NLP at the lipid-water interface. Therefore, caution has to be taken in EPR investigations just concluding from the mobility and polarity of a spin label being localised in a specific phase of a mixture without a proper reference system, since surface properties may influence the spin labels magnetic and dynamic properties in a dominant way.

The high pressure homogenisation apparently does not lead to the inclusion of DxPCA in the lipid matrix, which indicates an ordered matrix and expulsion of DxPCA to the surface during the preparation process.

Nevertheless, DxPCA is almost completely associated to the NLP and shows a NLP/water equilibrium distribution balanced towards the nanoparticles reflected by the *rt*-EPR of the undiluted NLP preparation, where only 2% free compound in aqueous solution could be found. This is probably promoted by the lipophilic properties of Dx and its low solubility in water.

Acknowledgment

The authors acknowledge support from Deutsche Forschungsgemeinschaft (DFG)/ German Research Foundation via CRC 1112, Projects A01 and B01.

Conflict of Interest

The authors state no conflict of interest.

References

1. Cevc, G., *Lipid vesicles and other colloids as drug carriers on the skin.* Advanced Drug Delivery Reviews, 2004. **56**(5): p. 675--711.
2. Lucks, J.S., R.H. Müller, and B. König, *Solid lipid nanoparticles (SLN) - an alternative parenteral drug carrier system.* Eur. J. Pharm. Biopharm., 1992. **38**: p. 33S.
3. Siekmann, B. and K. Westesen, *Submicron-sized parenteral carrier systems based on solid lipids.* Pharm. Pharmacol. Lett., 1992. **1**: p. 123–126.
4. Mäder, K. and W. Mehnert, *Solid lipid nanoparticles: production, characterization and applications.* Advanced drug delivery reviews, 2001. **47**(2-3): p. 165-96.
5. Müller, R.H., M. Radtke, and S.A. Wissing, *Solid lipid nanoparticles (SLN) and nanostructured lipid carriers (NLC) in cosmetic and dermatological preparations.* Advanced Drug Delivery Reviews, 2002. **54**: p. 131-155.
6. Müller, R.H., et al., *SOLID LIPID NANOPARTICLES (SLN) - AN ALTERNATIVE COLLOIDAL CARRIER SYSTEM FOR CONTROLLED DRUG-DELIVERY.* European Journal of Pharmaceutics and Biopharmaceutics, 1995. **41**(1): p. 62-69.
7. Kuo, Y.C. and H.H. Chen, *Entrapment and release of saquinavir using novel cationic solid lipid nanoparticles.* International Journal of Pharmaceutics, 2009. **365**(1-2): p. 206-213.
8. Jores, K., et al., *Investigations on the structure of solid lipid nanoparticles (SLN) and oil-loaded solid lipid nanoparticles by photon correlation spectroscopy, field-flow fractionation and transmission electron microscopy.* Journal of Controlled Release, 2004. **95**(2): p. 217-227.
9. Saupe, A., K.C. Gordon, and T. Rades, *Structural investigations on nanoemulsions, solid lipid nanoparticles and nanostructured lipid carriers by cryo-field emission scanning electron microscopy and Raman spectroscopy.* International Journal of Pharmaceutics, 2006. **314**(1): p. 56-62.
10. Westesen, K., H. Bunjes, and M.H.J. Koch, *Physicochemical characterization of lipid nanoparticles and evaluation of their drug loading capacity and sustained release potential.* Journal of Controlled Release, 1997. **48**(2-3): p. 223-236.
11. Jores, K., W. Mehnert, and K. Mäder, *Physicochemical Investigations on Solid Lipid Nanoparticles and on Oil-Loaded Solid Lipid Nanoparticles: A Nuclear Magnetic Resonance and Electron Spin Resonance Study.* Pharmaceutical Research, 2003. **20**(8): p. 1274-1283.
12. Lombardi Borgia, S., et al., *Lipid nanoparticles for skin penetration enhancement - Correlation to drug localization within the particle matrix as determined by fluorescence and parelectric spectroscopy.* Journal of Controlled Release, 2005. **110**(1): p. 151-163.
13. Müller, R.H., K. Mäder, and S. Gohla, *Solid lipid nanoparticles (SLN) for controlled drug delivery - A review of the state of the art.* European Journal of Pharmaceutics and Biopharmaceutics, 2000. **50**(1): p. 161-177.
14. Pardeike, J., A. Hommoss, and R.H. Müller, *Lipid nanoparticles (SLN, NLC) in cosmetic and pharmaceutical dermal products.* International journal of pharmaceutics, 2009. **366**(1-2): p. 170-84.
15. Andrade, L.M., et al., *Impact of lipid dynamic behavior on physical stability, in vitro release and skin permeation of genistein-loaded lipid nanoparticles.* European Journal of Pharmaceutics and Biopharmaceutics, 2014. **88**: p. 40-47.
16. Schäfer-Korting, M., W. Mehnert, and H.C. Korting, *Lipid nanoparticles for improved topical application of drugs for skin diseases.* Advanced Drug Delivery Reviews, 2007. **59**: p. 427-443.

17. Law, E.H. and M. Leung, *Corticosteroids in Stevens-Johnson Syndrome/toxic epidermal necrolysis: current evidence and implications for future research.* Ann Pharmacother, 2015. **49**(3): p. 335-42.
18. Marsh, D., *Polarity and permeation profiles in lipid membranes.* Proceedings of the National Academy of Sciences of the United States of America, 2001. **98**(14): p. 7777-7782.
19. Earle, K.A., et al., *250-GHz electron spin resonance studies of polarity gradients along the aliphatic chains in phospholipid membranes.* Biophysical journal, 1994. **66**(4): p. 1213-1221.
20. Hubbell, W.L. and C. Altenbach, *Investigation of structure and dynamics in membrane proteins using site-directed spin labeling.* Current Opinion in Structural Biology, 1994. **4**: p. 566-573.
21. Steinhoff, H.-J., et al., *High-field EPR studies of the structure and conformational changes of site-directed spin labeled bacteriorhodopsin.* Biochimica et Biophysica Acta - Bioenergetics, 2000. **1457**(3): p. 253-262.
22. Haag, S.F., et al., *Stabilization of reactive nitroxides using invasomes to allow prolonged electron paramagnetic resonance measurements.* Skin pharmacology and physiology, 2011. **24**(6): p. 312-21.
23. Honzak, L., M. Sentjurc, and H.M. Swartz, *In vivo EPR of topical delivery of a hydrophilic substance encapsulated in multilamellar liposomes applied to the skin of hairless and normal mice.* Journal of Controlled Release, 2000. **66**(2-3): p. 221-228.
24. Braem, C., et al., *Interaction of drug molecules with carrier systems as studied by parelectric spectroscopy and electron spin resonance.* Journal of controlled release : official journal of the Controlled Release Society, 2007. **119**(1): p. 128-35.
25. Haag, S.F., et al., *Skin penetration enhancement of core-multishell nanotransporters and invasomes measured by electron paramagnetic resonance spectroscopy.* International journal of pharmaceutics, 2011. **416**(1): p. 223-8.
26. Kempe, S., H. Metz, and K. Mäder, *Application of Electron Paramagnetic Resonance (EPR) spectroscopy and imaging in drug delivery research - Chances and challenges.* European Journal of Pharmaceutics and Biopharmaceutics, 2010. **74**(1): p. 55-66.
27. Unbehauen, M.L., et al., *Spin-labelled dexamethasone for Electron-Paramagnetic Resonance (EPR) Spectroscopy.*, 2016 (in preparation).
28. Weidinger, A., et al., *Atomic nitrogen in C60: N@C60.* Applied Physics a-Materials Science & Processing, 1998. **66**: p. 287-292.
29. Stoll, S. and A. Schweiger, *EasySpin, a comprehensive software package for spectral simulation and analysis in EPR.* J Magn Reson, 2006. **178**(1): p. 42-55.
30. Kawamura, T., S. Matsunami, and T. Yonezawa, *Solvent Effects on the g-Value of Di-t-butyl Nitric Oxide.* Bulletin of the Chemical Society of Japan 1967. **40**(5): p. 1111-1115.
31. Owenius, R., et al., *Influence of Solvent Polarity and Hydrogen Bonding on the EPR Parameters of Nitroxide Spin label studied by 9-GHz and 95 GHz EPR Spectroscopy and DFT Calculations.* J. Phys Chem 2001. **105**(49): p. 10967-10977.
32. Marsh, D., *Spin-Label EPR for Determining Polarity and Proticity in Biomolecular Assemblies: Transmembrane Profiles.* Appl Magn Reson, 2010. **37**(1-4): p. 435-454.
33. Kim, D.H. and D.C. Martin, *Sustained release of dexamethasone from hydrophilic matrices using PLGA nanoparticles for neural drug delivery.* Biomaterials, 2006. **27**(15): p. 3031-7.
34. Saeidpour, S., et al., *Localization of dexamethasone within dendritic core-multishell (CMS) nanoparticles using multifrequency electron paramagnetic resonance spectroscopy (EPR).* European Journal of Pharmaceutics and Biopharmaceutics, 2016. **,** http://dx.doi.org/10.1016/j.ejpb.2016.10.001.

35. Freed, J.H., *Theory of Slow Tumbling ESR Spectra for Nitroxides.* Spin labeling theory and application, 1976. **Academic Press Inc.**(Edited by L.J. Berliner).
36. Sivaramakrishnan, R., et al., *Glucocorticoid entrapment into lipid carriers--characterisation by parelectric spectroscopy and influence on dermal uptake.* J Control Release, 2004. **97**(3): p. 493-502.
37. Lukowski, G. and J. Kasbohm, *Energy Dispersive X-ray analysis of loaded solid lipid nanoparticles.* . J Proceedings - 28th International Symposium on Controlled Release of Bioactive Materials and 4th Consumer & Diversified Products Conference, San Diego, CA, United Staes, 2001: p. 516-517.

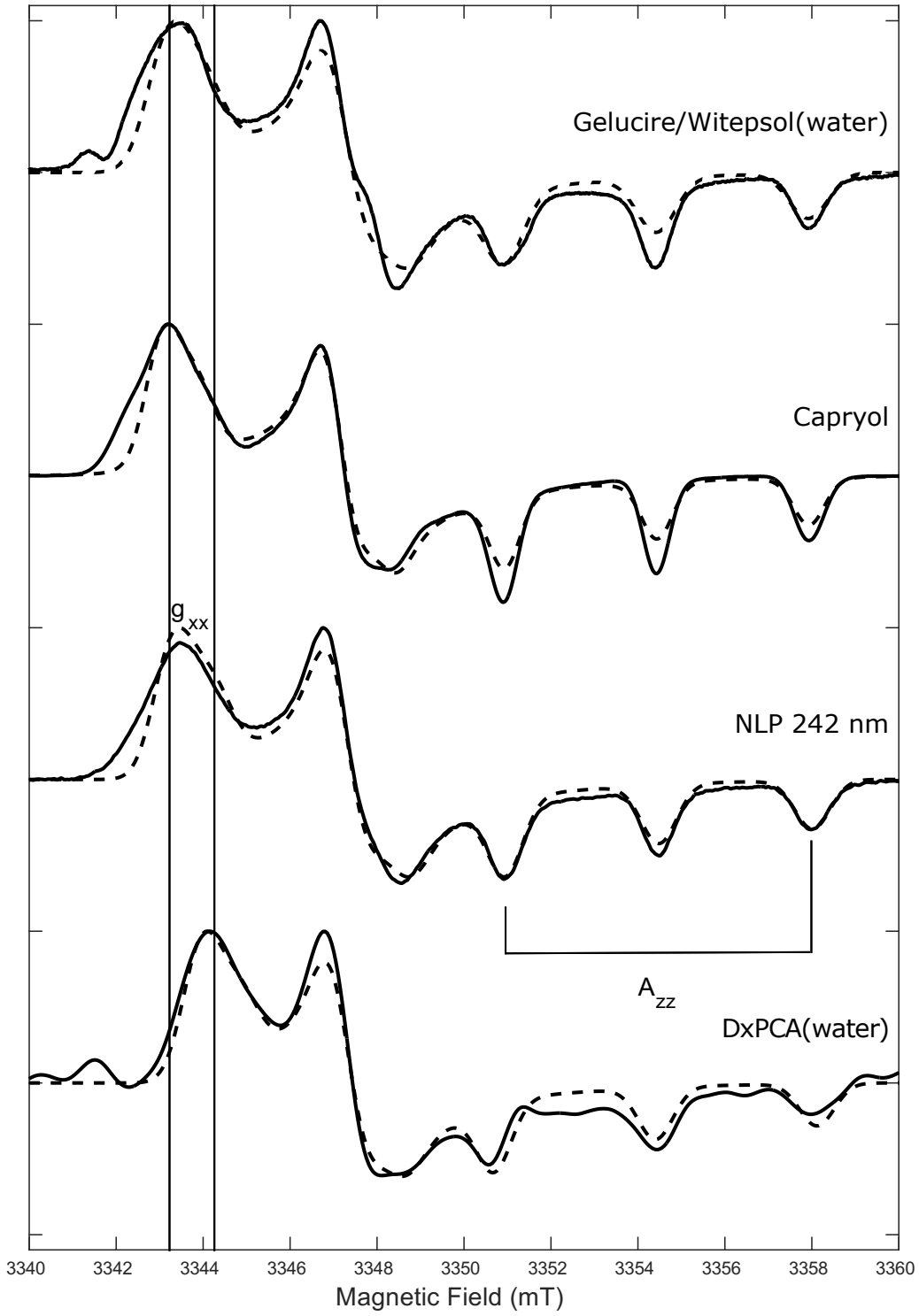

Figure 1

Cryogenic Temperature EPR Spectra at 80 K for DxPCA measured at W-band in different components/ solutions (solid line: experiment, dashed line: simulation): Gelucire/ Witepsol(water), Capryol, NLP solution (242 nm) and DxPCA(water); exp. Parameters: field-swept echo spectra, pseudo modulation 5 G; *cw*-EPR for NLP (242 nm): microwave power 5 nW, modulation amplitude 5 G.

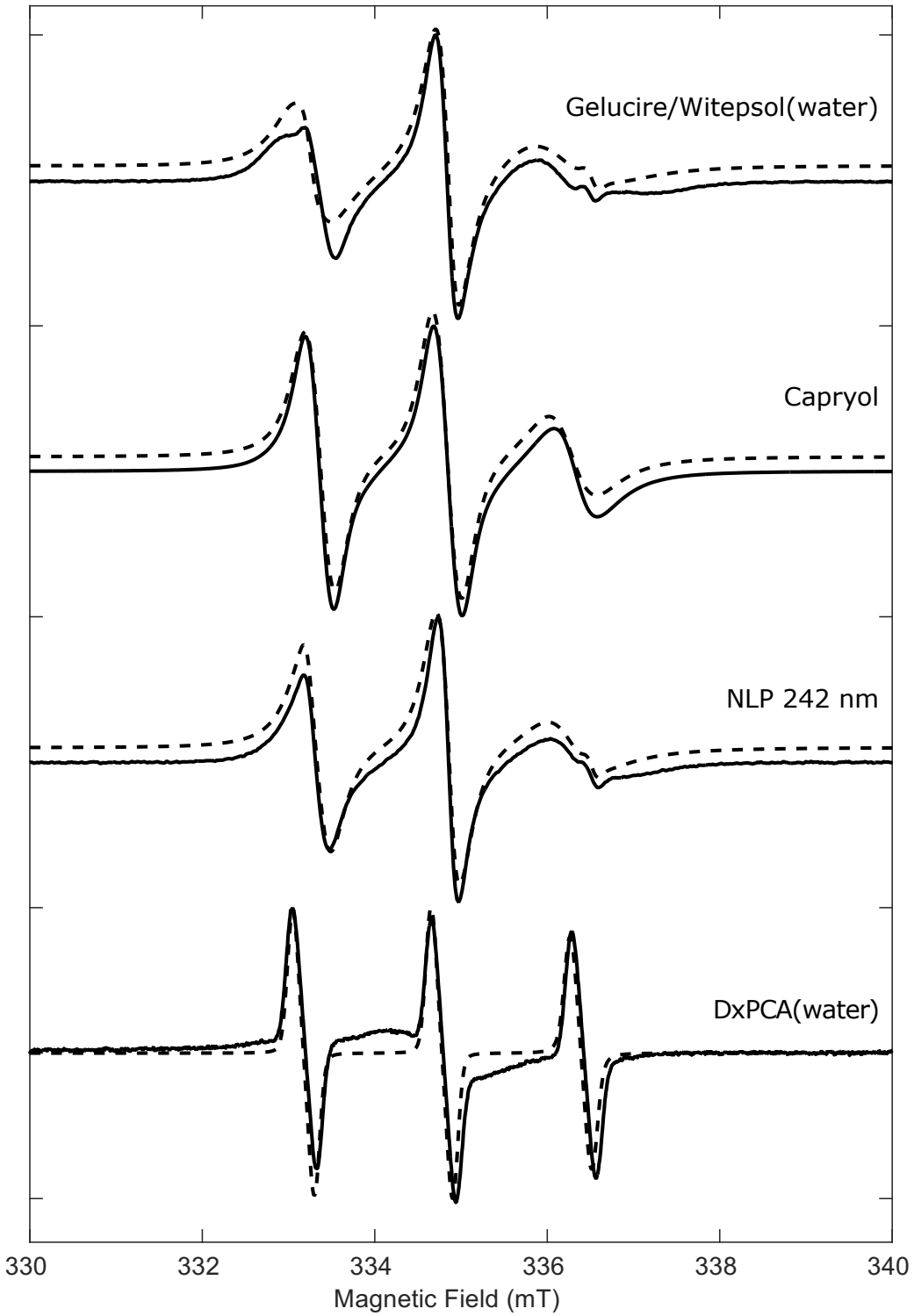

Figure 2

X-band EPR spectra of DxPCA in NLP, in individual lipids and water at room temperature (Solid line: experiment, dashed line: simulation); experimental parameters for the different formulations: microwave power 1 mW, modulation amplitude 1 G for DxPCA in water, for the other spectra 3 G.

Supplemental data

Table S1

Physical properties of unlabeled and spin-labelled Dexamethasone

	Dexamethasone	Dexamethasone-PCA
Molecular weight [g/mol]	392.47	578.7
solubility in water [mol/l]	$2.3 \cdot 10^{-4}$	$2 \cdot 10^{-6}$
Partition coefficient, $\log(P_{octanol/water})$	1.83-1.89	1.87-1.90[1]

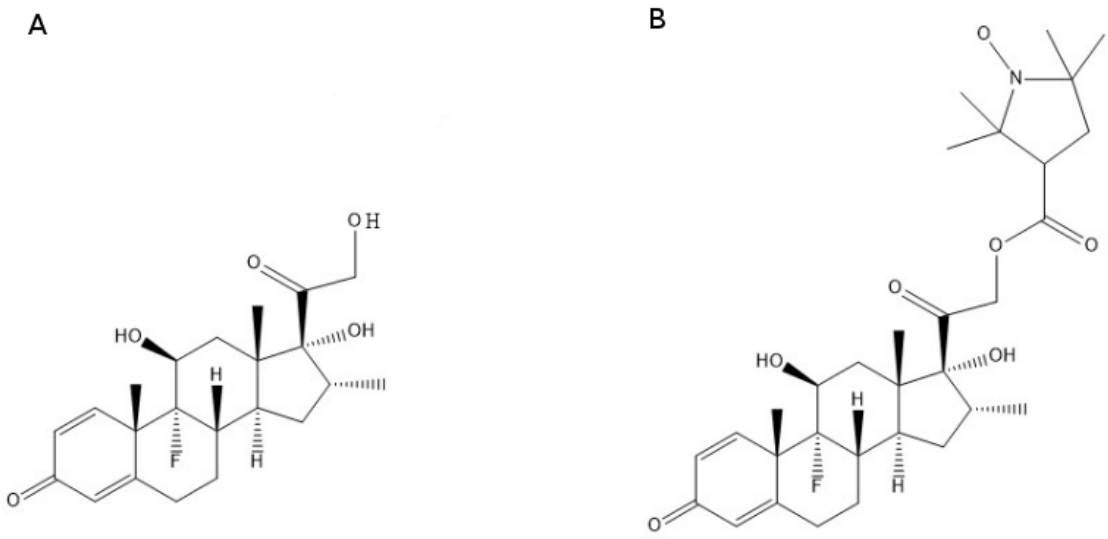

Figure S1

Chemical structures of (A) Dexamethasone and (B) PCA-spinlabelled Dexamethasone (M_{PCA}=186.23 g/mol).

[1] Determined by the shaked flask method, quantitation by EPR

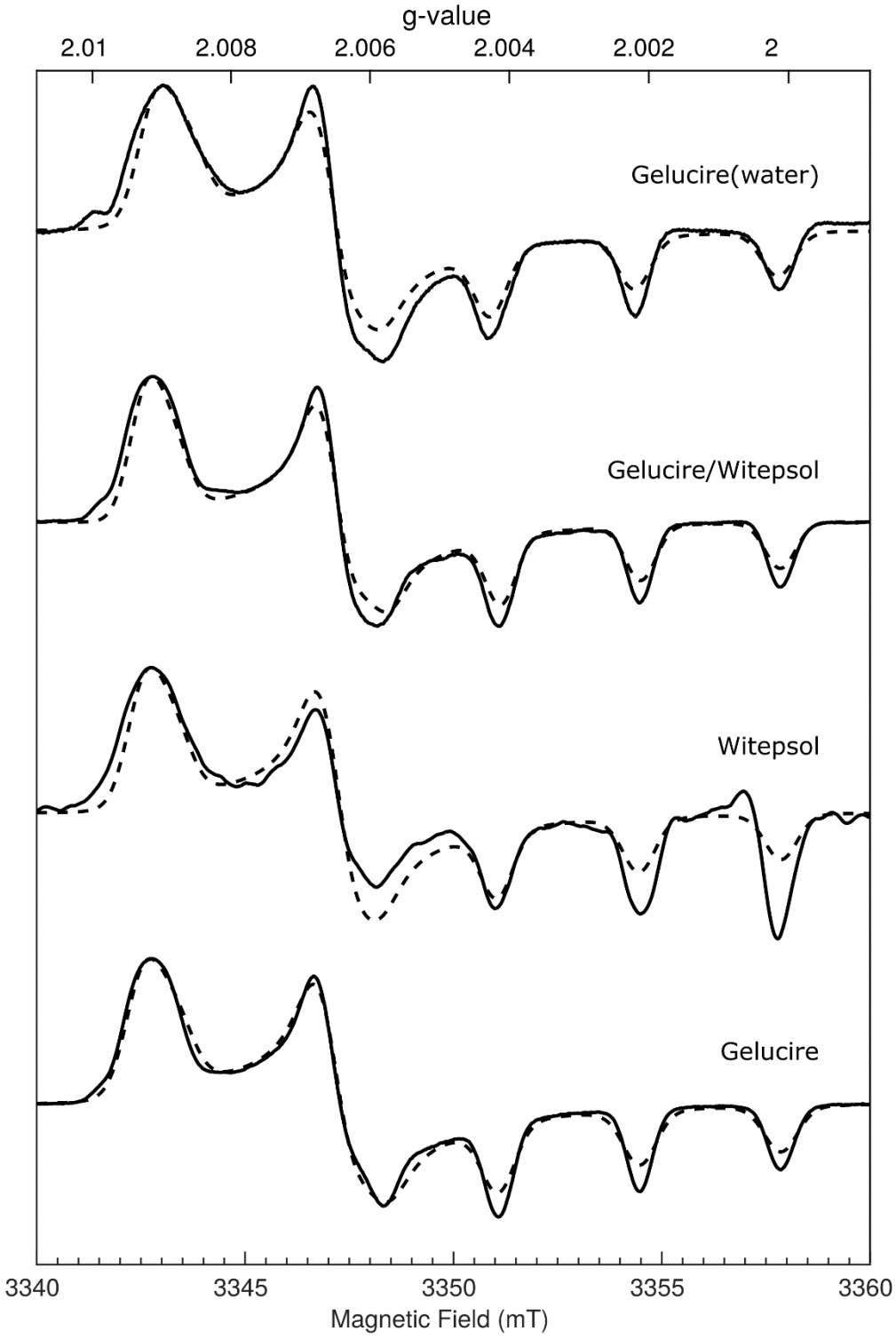

Figure S2

EPR spectra of DxPCA at 80 K in different lipid compositions at W-band, solid line: experiment, dashed line: simulation , exp. parameters: Gelucire/ Witepsol, Witepsol and Gelucire) field sweep echo, pseudo modulation amplitude 5 G, Gelucire(water): microwave power 5 nW,modulation amplitude 5 G, modulation frequency 100 kHz.

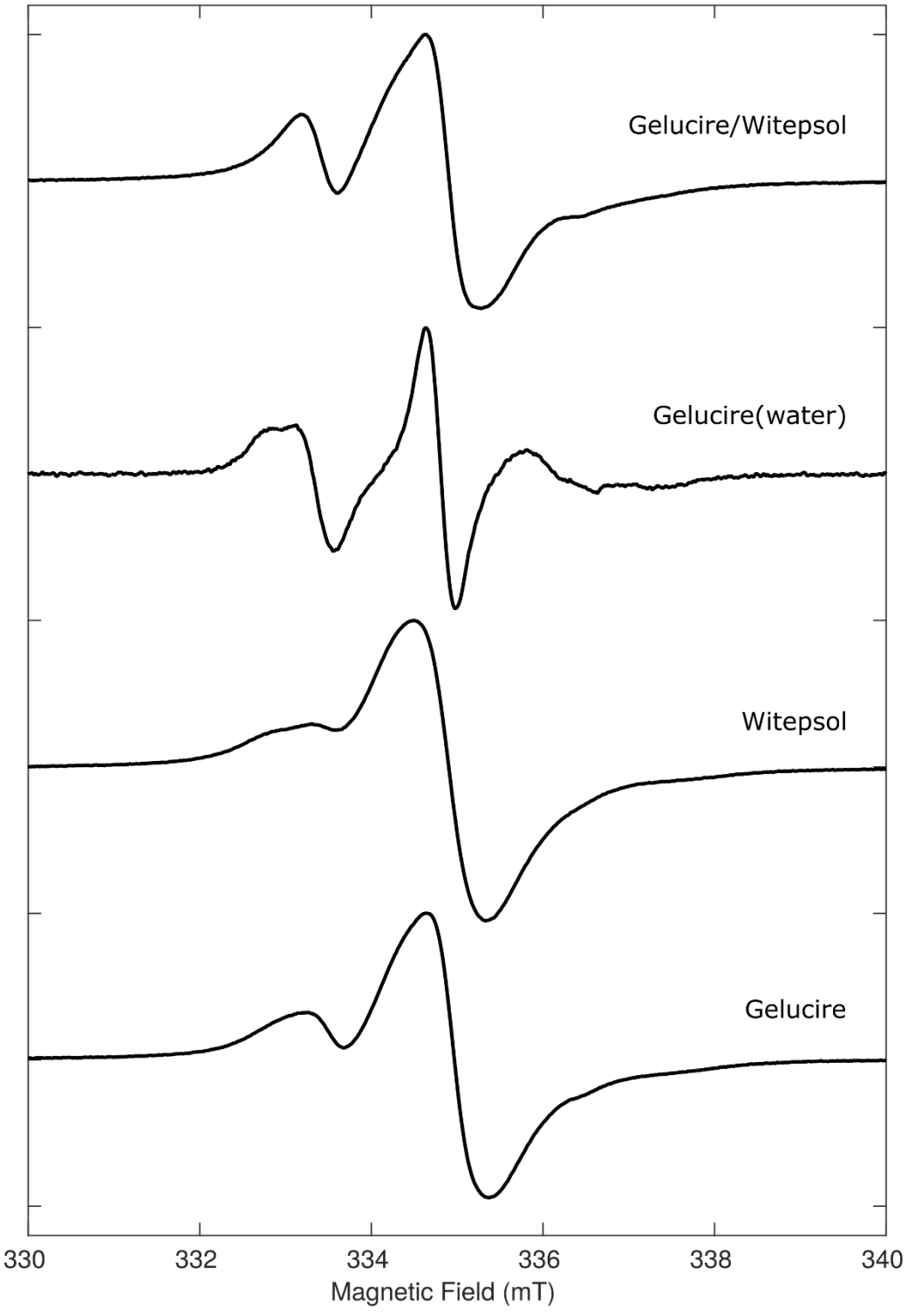

Figure S3

X-band EPR spectra of DxPCA in NLP, in individual lipids and lipid mixtures dispersed in water at room temperature; experimental parameters for the different formulations: microwave power 1.0 mW, modulation amplitude 3 G, modulation frequency 100 kHz.

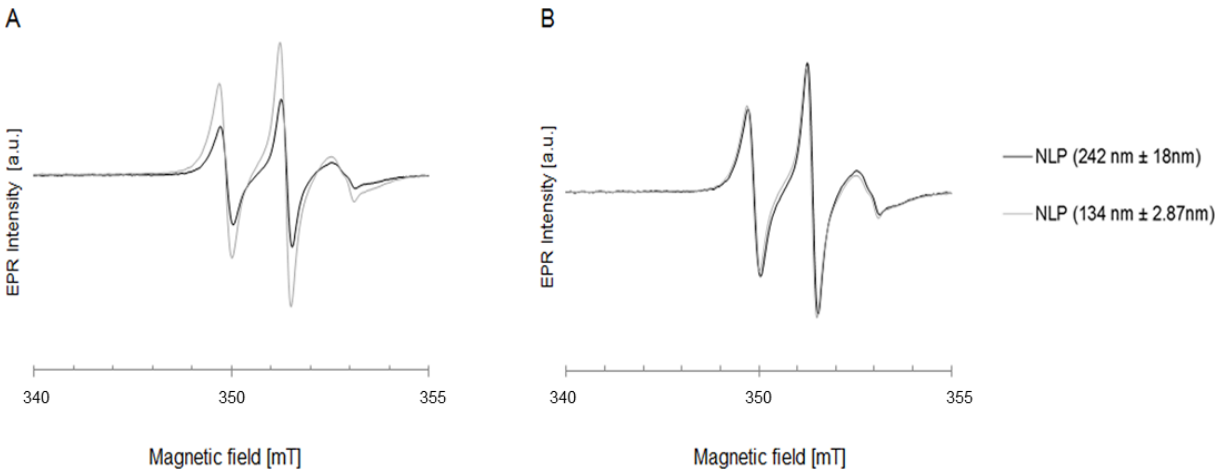

Figure S4

X-band EPR spectra of DxPCA loaded to NLP with different sizes (242 nm ± 18 nm, 134 nm ± 3 nm) at room temperature. A) unscaled spectra from solutions of the same concentration (100 mg/ml); B) scaled EPR spectra, which show the same lineshape for both particle sizes. exp. parameters: modulation frequency 100 kHz, modulation amplitude 2 G, microwave power 1.3 mW

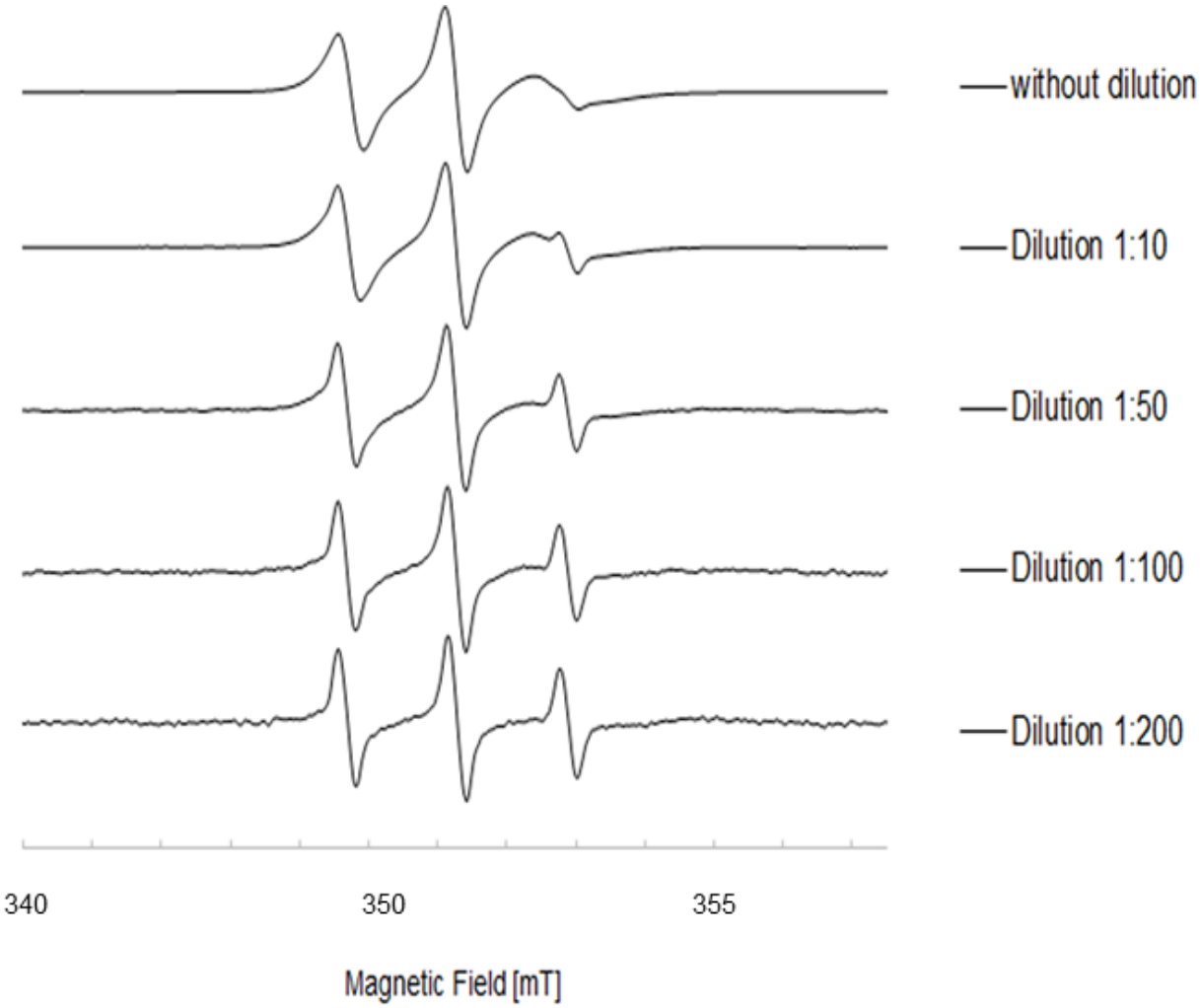

Figure S5

X-band EPR spectra DxPCA loaded to NLP after dilution with aqueous solution (Dilution steps: 1:10, 1:50, 1:100, 1:200) at room temperature. All X-band EPR spectra were scaled to the size of spectrum without dilution. exp. parameters: modulation frequency 100 kHz, modulation amplitude 2 G, microwave power 1.3 mW

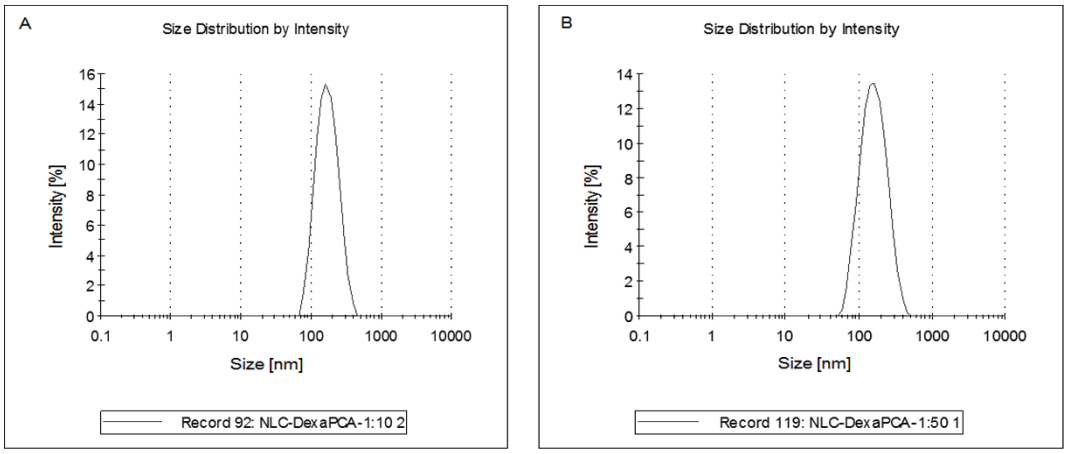

Figure S6

Dynamic light scattering measurements of DxPCA loaded NLP after dilution with water, A) Size distribution of the NLP after a dilution 1:10 with aqueous solution; B) Size distribution of NLP after a dilution 1:50 with aqueous solution.